

Dehydration and reduction of synthetic garnierite

J. J. F. SCHOLTEN

Department of Chemical Technology, Delft University of Technology, Julianalaan 136, Delft-2208, The Netherlands

A. M. KIEL

Central Laboratory, DSM, Geleen, The Netherlands

The morphology of synthetic garnierite, $\text{Ni}_3(\text{OH})_4 \cdot \text{Si}_2\text{O}_5$, has been studied by electron microscopy. The layer structure of the hollow garnierite needles has been made visible and the observed layer distance is in accordance with the X-ray result. Synthetic garnierite, totally dehydrated above 500°C , appears to be pseudomorphous with garnierite. Total reduction of the dehydrated product in hydrogen yields porous nickel-on-silica in which the small nickel crystallites are only partly accessible to hydrogen chemisorption.

1. Introduction

Among the hydrated minerals, chrysotile, $\text{Mg}_3(\text{OH})_4 \cdot \text{Si}_2\text{O}_5$, and garnierite, $\text{Ni}_3(\text{OH})_4 \cdot \text{Si}_2\text{O}_5$, occupy a special place because, at first sight, their morphology is not in accordance with their crystallographic structure; both the natural and synthetic forms occur in bundles of parallel fibres, whereas X-ray studies disclose a layered structure.

At first, Warren and Bragg [1], on the grounds of their X-ray study of natural chrysotile, considered the structure to be built up of chains having the composition Si_4O_{11} and, in between the sets of chains, sections composed of Mg and OH. Such a structure would be in accordance with the fibrous nature of the material. Later, Aruja [2] and Whittaker [3] showed that a layered structure would fit in better with the composition and the diffraction pattern than the previously proposed chain structure.

The layered structure of chrysotile and garnierite resembles that of kaolinite, $\text{Al}_2(\text{OH})_4 \cdot \text{Si}_2\text{O}_5$. In the silica layers, every SiO_4 tetrahedron is bound to three others, sharing one angular point with each of them, and in this way $\text{Si}_2\text{O}_5^{2-}$ plates are formed. These plates are covered with $\text{Mg}_3(\text{OH})_4^{2+}$ layers which, in turn, are overlaid with a second $\text{Si}_2\text{O}_5^{2-}$ layer, and so on.

In nature three polymorphs of chrysotile are found, namely clino-chrysotile, ortho-chrysotile

and para-chrysotile. Whittaker showed this polymorphism to be linked with three different positions of the Mg atoms in the structure [3, 4].

The discovery that chrysotile has a layered structure raised the question as to how this structure can be reconciled with the highly perfect fibrous character of the material. Pauling [5] in 1930 already suggested that if a magnesium analogue of kaolinite should exist, it would have curved layers, owing to the misfit between the two halves of the layer. In 1950, Bates *et al.* [6] advanced electron microscopic evidence showing that this is indeed the case; the layers are cylindrically curved around the fibre axis. Owing to this circular (or spiral) structure, hollow needles are formed, varying in length, wall thickness and internal diameter; the wall of the average needle consists of about ten double layers.

The $\text{Mg}_3(\text{OH})_4^{2+}$ layer is bound in two different ways to the three oxygen atoms forming the basis of the SiO_4 tetrahedrons in the next $\text{Si}_2\text{O}_5^{2-}$ layer; some of the hydroxyl groups are located between the three basic oxygen atoms, others are bound to one of the oxygen atoms via a hydrogen bridge. The proportion in which these two binding modes occur depends on the curvature of the layers, which is, of course, a function of the distance of the layer from the needle axis. Hence, this interlayer disorder,

which also follows from crystallography, is directly linked with the cylindrical structure of chrysotile.

Chrysotile and its nickel isomorph, garnierite, may also be obtained synthetically [7]. According to Spangenberg [8], natural and synthetic garnierite have the same crystallographic structure as mineral chrysotile.

The present article presents an electron microscopical study on the morphologies of synthetic chrysotile and, particularly, garnierite. In the case of garnierite, the layered structure of the needle walls can be made visible. The morphology of totally dehydrated garnierite will be discussed, and it will be shown that the dehydrated material is pseudomorphous with garnierite. Finally, the effects of total dehydration followed by reduction will be considered.

2. Experimental

Chrysotile was prepared according to the specifications by Noll *et al.* [7]. A solution of 102 g $\text{MgCl}_2 \cdot 6\text{H}_2\text{O}$, reagent grade, in 200 ml distilled water, was mixed with a solution of 95 g $\text{Na}_2\text{Si}_2\text{O}_3 \cdot 9\text{H}_2\text{O}$, prepared by dissolving silica (trade mark "Aerosil" of Degussa, Germany) in sodium hydroxide, and with 14 g sodium hydroxide, reagent grade, dissolved in 400 ml distilled water. The quantities were so chosen as to correspond with the stoichiometry of chrysotile. The mixture was vigorously stirred, resulting in precipitation of a white gel-like substance. About 600 ml of the solution was placed in a nickel crucible of 100 cm^3 volume, which was mounted in a 1 litre autoclave filled with 400 ml distilled water. After closing the autoclave, the temperature was raised to 295°C over 3 h; the final steam pressure was then $\sim 87 \text{ kg cm}^{-2}$. After 8 h reaction, the autoclave was slowly cooled down and opened. The gel-like product was washed several times with distilled water to remove all chlorine, and subsequently with 96% ethanol. After evaporation of the alcohol at 100°C, the sample was dried at 110°C.

Garnierite was prepared in a similar way, with nickel sulphate, reagent grade from BDH, being used instead of magnesium chloride. In the dry condition, garnierite has a pale green colour, and the needles cohere to some degree. Scanning electron microscopy showed, however, that the parallel coherence of the needles is not as strong as in asbestos.

Electron micrographs were taken with a Philips EM 300. Suspensions of the needles in

alcohol were brought onto a small-mesh wire netting coated with a carbon film. The needle-wall structure was made visible by embedding the garnierite in methylmethacrylate and sectioning it into coupes of less than 50 nm thickness by means of an ultramicrotome. Lengths were calibrated by means of a Rowland grid of 2160 lines mm^{-1} .

The dehydration and reduction of garnierite was studied thermogravimetrically in a Mettler Thermoanalyzer, type No. 1, in a stream of highly purified argon.

The crystallographic structure and its fading-away during dehydration, was studied in a temperature-programmed Guiner-Lenné camera [9]. The temperature was gauged by adding some K_2SO_4 , which has a transition point at 588°C.

The total accessible surface area was determined from the physical adsorption isotherm of nitrogen at -196°C , in a classical BET apparatus. The cross-sectional area of the nitrogen molecule was taken to be 1.62 nm.

The free-nickel surface area of totally dehydrated and reduced garnierite was calculated from the extent of a monolayer of chemisorbed hydrogen. The chemisorption isotherm, measured at 20°C in the BET apparatus, showed an initial steep rise, and started to run parallel to the pressure axis at 1 cm Hg pressure, which indicates full coverage. In the calculation of the free-metal surface area, it was supposed that every surface metal atom chemisorbs one hydrogen atom, and that the nickel crystallites expose 25% (100), 5% (110) and 70% (111) planes. This distribution of the crystallographic planes has been adopted from Sundquist's EM observations [10] of the surface of small fcc gold crystals. On this basis, 1 cm^3 hydrogen (NTP) chemisorbed corresponds to 3.06 m^2 free-nickel surface area.

3. Results

3.1. Morphology of chrysotile and garnierite

Fig. 1 represents an electron micrograph of a suspension of our synthetic chrysotile preparation. The hollow-needle shape is very evident. In some places where the needles are disposed perpendicularly to the plane of observation, the circular shape of the pores is clearly visible. From 250 countings we found a mean internal radius of the needles of $3.2 \pm 1.0 \text{ nm}$, and a mean external radius of $14.1 \pm 1.2 \text{ nm}$.

A micrograph of a suspension of synthetic garnierite is represented in Fig. 2. It is seen that



Figure 1 Electron micrograph of synthetic chrysotile.

in accordance with Noll and Kircher's observations [11] the crystallites have the same hollow-needle shape as synthetic chrysotile; however, irregular crystal growth and growth defects, as described for natural chrysotile asbestos by Keiji Yada [12], are much more frequent than in the latter. From 250 countings we found that the mean internal radius of the needles is

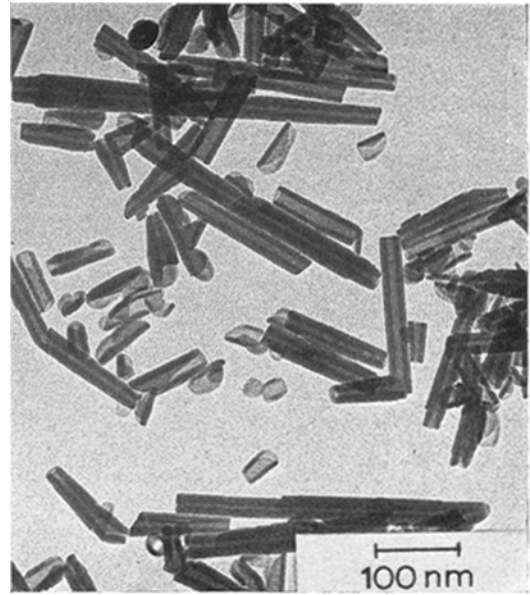


Figure 2 Electron micrograph of synthetic garnierite.

significantly larger than in chrysotile, i.e. 4.5 ± 1.0 nm, whereas the mean external radius is of the same order, i.e. 13.9 ± 1.2 nm. Both in chrysotile and in garnierite the mean needle length was of the order of 170 nm.

Unlike chrysotile, garnierite contains two types of crystals; hollow needles, and horseshoe-shaped crystals having a larger mean "radius" and somewhat thinner walls. A good example of

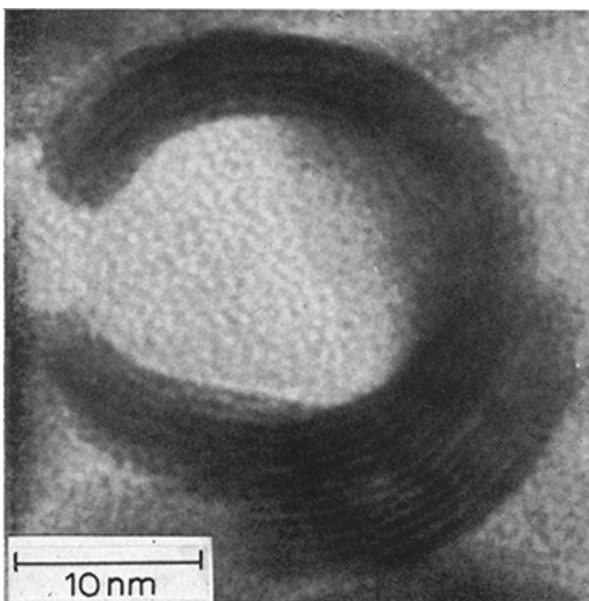


Figure 3 Electron micrograph of a 50 nm microtome section of synthetic garnierite showing a horseshoeshaped crystal.

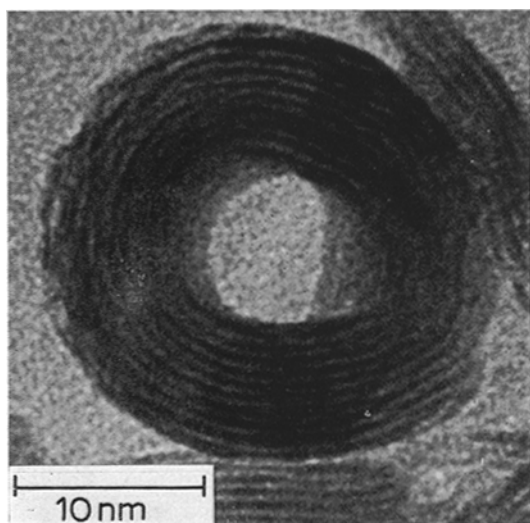


Figure 4 Electron micrograph of a 50 nm microtome section of synthetic garnierite showing the layered structure of the needle walls.

a horseshoe-shaped crystal is illustrated in Fig. 3 which shows a high-resolution micrograph of a 50 nm microtome section of synthetic garnierite.

Fig. 4 shows a high-resolution micrograph of a hollow-needle crystal, viewed in the direction of the needle axis (sectioning technique). As in Fig. 3, the layered structure is clearly visible, owing to the fact that the 26 electrons of the Ni^{2+} ions have much more scattering power than the 10 electrons of the Mg^{2+} ions in chrysotile, where the wall structure is much less in evidence.

From Figs. 3 and 4 we calculated the mean layer distance in the walls of the garnierite needles to be 0.7 ± 0.04 and 0.72 ± 0.04 nm respectively, which values come very near to the layer distance found crystallographically (0.73 nm). Keiji Yada [12], applying high-resolution electron microscopy, found a layer distance of 0.73 nm in natural chrysotile asbestos.

3.2. Dehydration of garnierite

A small sample of garnierite was examined under a stream of pure argon in the Mettler Thermoanalyzer at a heating rate of 4°C min^{-1} . The percentage weight change as a function of temperature is presented in Fig. 5. Between room temperature and 100°C , physically adsorbed and capillary condensed water desorbs. Above that temperature, a strong weight change sets in which, passing through a maximum around 500°C , is related to the desorption of chemically bound water (dehydration of hydroxyl groups in

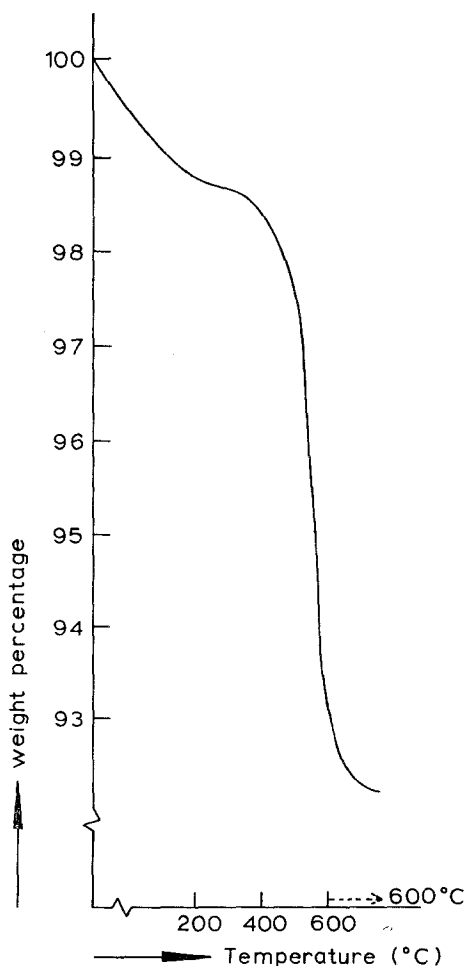


Figure 5 Dehydration of synthetic garnierite. The percentage weight change is plotted as a function of temperature. Heating rate: 4°C min^{-1} in argon.

the lattice). The total observed weight change is in accordance with the stoichiometry of the reaction:



An analogous result was found by Noll [13] when dehydrating synthetic chrysotile. Here constitutional water desorbed between 500 and 550°C .

Fig. 6 is a micrograph of a preparation totally dehydrated in the Mettler Thermoanalyzer. It is worthy to note that, although the material in question is clearly a nickel oxide–nickel silicate mixture, the shape of the hollow needles and horseshoe crystals of garnierite has been completely preserved.

In a parallel experiment, part of the garnierite sample was heated in the temperature-pro-



Figure 6 Electron micrograph of totally dehydrated synthetic garnierite. Maximum dehydration temperature: 600°C.

grammed Guinier-Lenné camera at a heating rate of 50°C h⁻¹ to the final level of 650°C, in a stream of pure nitrogen. The initial diffraction pattern was in accordance with the X-ray powder data of garnierite published by Feitknecht and Berger [14]. At 460 ± 15°C, the characteristic diffraction lines of garnierite have already disappeared, to be replaced by vague broad lines corresponding with the spacings $d = 0.445, 0.260, 0.240$ and 0.151 nm. Comparison of these figures with those found by Coenen [15] for finally divided nickel oxide and nickel silicate, suggests that we are dealing here with a mixture of said two compounds.

It follows from the foregoing that the sample represented by the micrograph of Fig. 6 was totally free of garnierite, but nevertheless had the same morphology. So we are concerned here with an interesting case of pseudomorphosis. There are, however, some indications showing that the dimensions of the needles have changed owing to dehydration; from 45 countings we found a mean internal diameter of 5.5 ± 1.8 nm (hydrated: 4.5 ± 1.0 nm), whereas the mean external radius was 12.5 ± 2.5 nm (hydrated: 13.9 ± 1.2 nm). That the morphology has been preserved also follows from the fact that the BET surface areas before and after total dehydration were practically identical, i.e. ~ 87 m² g⁻¹.

3.3. Reduction of garnierite

Reduction of garnierite in a stream of nitrogen containing 0.1% hydrogen became measurable at 580°C. Complete reduction, effected in a stream of pure hydrogen at 600°C, took 72 h. After 24 h evacuation at 550°C, the hydrogen chemisorption isotherm at room temperature was measured. Calculation from the amount of chemisorbed hydrogen showed the free-nickel surface area to be 42.9 m² Ni per g Ni. On the assumption that the nickel particles are totally accessible and spherically shaped, the mean volume-surface diameter $\bar{d}_{v.s.}$ (sphere) can be calculated from:

$$\bar{d}_{v.s.}(\text{sphere}) = 6V/S \quad (1)$$

where V is the volume of 1 g of nickel and S the surface area per g of nickel.

Assuming the nickel crystallites to be bound to the silica surface in the form of hemispheres, which is in analogy to Coenen and Linsen's findings for nickel-on-silica catalysts [16], we have:

$$\bar{d}_{v.s.}(\text{hemispheres}) = 3V/S. \quad (2)$$

From the free-nickel surface area, $\bar{d}_{v.s.}$ (sphere) is found to be 15.7 nm, whereas $\bar{d}_{v.s.}$ (hemisphere) is 7.85 nm.

Next the reduced garnierite sample was passivated in a stream of nitrogen containing 0.02 to 0.1% oxygen, and part of it was examined under the electron microscope. The result is given in Fig. 7 in which the original needle shape of the garnierite can no longer be distinguished and a large number of nickel crystallites on silica is observed instead.

The mean volume-surface diameter, defined by

$$\bar{d}_{v.s.}(\text{EM}) = \frac{\sum n_i d_i^3}{\sum n_i d_i^2} \quad (3)$$

where n_i is the number of crystallites of diameter d_i , is found by a count of the diameters of 288 crystallites in the electron micrographs. $\bar{d}_{v.s.}$ (EM) revealed to be 6.9 ± 1.5 nm, which value agrees much better with that found from the hemisphere model proposed by Coenen; than with the sphere model. It is evident, therefore, that just as in nickel-on-silica catalysts, the nickel crystallites are fixed to the silica carrier, and that the part of the nickel attached to silica is not accessible to hydrogen chemisorption.

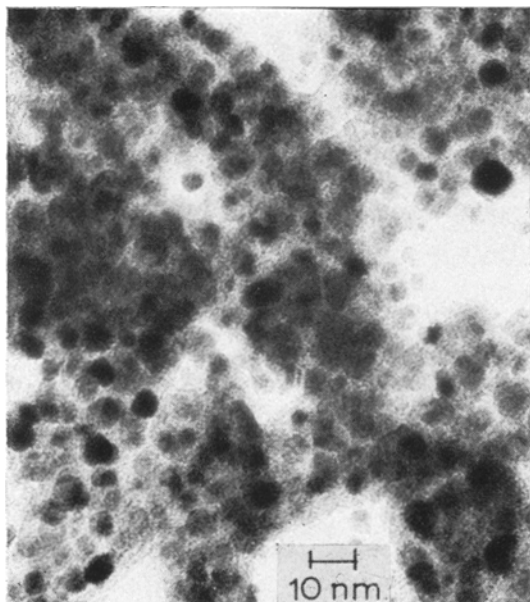


Figure 7 Electron micrograph of totally dehydrated and reduced garnierite.

4. Conclusions

Inspection of a large number of micrographs like those in Fig. 4, reveals that circular growth of the needles is more likely than spiral growth.

Micrographs like the one presented in Fig. 3, make the structure of the horseshoe-shaped crystallites very clear. The growth mechanism of this type of crystallites is probably as follows.

The first bent layer starts growing, but at a given moment, when it has not yet closed to form a cylinder, the second layer, growing along the convex side, arrives at the edge of the first layer, where it changes its direction of growth and continues growing along the concave innerside of the first layer. The third and following layers show the same behaviour.

We fully subscribe Pauling's explanation of the curved form of the layers (see Introduction), which has been confirmed by the crystallographic work by Whittaker [3, 4]. In a foregoing publication [17] we supported the interpretation given by Keiji Yada [12], who ascribed the curved form of the needles to growth defects initiated by contaminating ions. Our opinion at that time was based on the crystallographic structure of chrysotile presented by Warren and

Bragg [1], which conflicts with Pauling's idea. However, this structure has now been rendered out of date by Whittaker's work.

The pseudomorphosis demonstrated for totally dehydrated garnierite cannot be made comprehensible very easily. We found that the density of garnierite, dried at room temperature, is $0.26 \text{ cm}^3 \text{ g}^{-1}$ (helium pycnometry). The calculated density of the dehydration product being $0.21 \text{ cm}^3 \text{ g}^{-1}$, the volume change by dehydration is only $0.05 \text{ cm}^3 \text{ g}^{-1}$. This small volume change, together with the stable hollow-tube structure of the needles, will certainly contribute to the preservation of the hollow-needle form.

Acknowledgements

Thanks are due to Mrs F. Jaminon, Mrs L. de Wit, Mr J. A. Konvalinka and Mr J. Teunisse, for helpful discussions, and experimental and mathematical assistance. Dr J. W. Visser of the "Technisch Physische Dienst" TNO, Delft, performed the X-ray work.

References

1. B. E. WARREN and W. L. BRAGG, *Z. Kristallogr.* **76** (1930) 201.
2. E. ARUJA, Ph.D. Thesis, Cambridge (1943).
3. E. J. W. WHITTAKER, *Acta Cryst.* **6** (1953) 747.
4. *Idem, ibid* **9** (1956) 855, 862, 865.
5. L. PAULING, *Proc. Nat. Acad. Sci. Wash.* **16** (1930) 578.
6. T. F. BATES, L. B. SAND and J. F. MINK, *Science* **111** (1950) 512.
7. W. NOLL, H. KIRCHER and W. SYBERTZ, *Kolloid Z.* **157** (1958) 1.
8. K. SPANGENBERG, *Naturwissensch.* **26** (1938) 578.
9. U. H. LENNÉ, *Z. Kristallogr.* **116** (1961) 189.
10. B. E. SUNDQUIST, *Acta Met.* **12** (1964) 67.
11. W. NOLL and H. KIRCHER, *Naturwissensch.* **39** (1952) 233.
12. KEIJI YADA, *Acta Cryst.* **23** (1967) 704.
13. W. NOLL, *Z. Anorg. Chem.* **261** (1950) 1.
14. W. FEITKNECHT and A. BERGER, *Helv. chim. acta* **25** (1942) 1534.
15. J. W. E. COENEN, Thesis Delft University, Delft (1958), editor Excelsior, The Hague, 1958.
16. J. W. E. COENEN and B. G. LINSEN, "Physical and Chemical Aspects of Adsorbents and Catalysts" edited by B. G. Linsen (Academic Press, London and New York, 1970) Chapter 10.
17. J. J. F. SCHOLTEN, A. M. BEERS and A. M. KIEL, *J. Catalysis* **36** (1975) 23.

Received 4 December 1974 and accepted 7 January 1975.